Chapter 8

Functional profiling of receptor tyrosine kinases and downstream signaling in human chondrosarcomas identifies pathways for rational targeted therapy

This chapter is based on the manuscript: Zhang Y-X, van Oosterwijk JG, Sicinska E, Moss S, Remillard SP, Wezel T, Bühnemann C, Hassan AB, Demetri GD, Bovée JVMG, Wagner AJ. *Clin Cancer Res. 2013;19(14):3796-807*

Translational Relevance

Chondrosarcomas are notoriously resistant to conventional chemotherapy. There is an urgent need to identify therapeutic targets and to develop novel treatment strategies for this disease.
We found multiple RTKs to be activated in chondrosarcoma cells and to have critical roles in mediating cell growth. Strong phosphorylation of S6 was detected in 69% of conventional chondrosarcoma and 44% of dedifferentiated chondrosarcoma clinical samples and is likely due to RTK activation. Inhibition of PI3K and mTOR, signaling proteins downstream of RTKs and upstream of S6, potently blocked the growth of chondrosarcoma cells *in vitro* and *in vivo*.
NRAS mutations were identified in 12% of conventional central chondrosarcoma tumor tissues. An *NRAS* mutation-harboring chondrosarcoma cell line was sensitive to treatment with a MEK inhibitor.
Our findings provide new insights into the genetics and the heterogeneity of chondrosarcomas, and have implications for the clinical development of PI3K/mTOR or MEK inhibitors in this disease.

Abstract

Chondrosarcomas are notoriously resistant to cytotoxic chemotherapeutic agents. We sought to identify critical signaling pathways that contribute to their survival and proliferation, and which may provide potential targets for rational therapeutic interventions.
Activation of receptor tyrosine kinases (RTKs) was surveyed using phospho-RTK arrays. S6 phosphorylation and *NRAS* mutational status were examined in chondrosarcoma primary tumor tissues. Small interfering RNA or small molecule inhibitors against RTKs or downstream signaling proteins were applied to chondrosarcoma cells and changes in biochemical signaling, cell cycle, and cell viability were determined. *In vivo* anti-tumor activity of BEZ235, a phosphoinositide-3-kinase (PI3K)/mammalian target of rapamycin (mTOR) inhibitor, was evaluated in a chondrosarcoma xenograft model.
Several RTKs were identified as critical mediators of cell growth, but the RTK dependencies varied among cell lines. In exploration of downstream signaling pathways, strong S6 phosphorylation was found in 69% of conventional chondrosarcomas and 44% of dedifferentiated chondrosarcomas. Treatment with BEZ235 resulted in dramatic reduction in the growth of all chondrosarcoma cell lines. Tumor growth was similarly inhibited in a xenograft model of chondrosarcoma. In addition, chondrosarcoma cells with an *NRAS* mutation were sensitive to treatment with a MEK inhibitor. Functional *NRAS* mutations were found in 12% of conventional central chondrosarcomas.
RTKs are commonly activated in chondrosarcoma, but because of their considerable heterogeneity, targeted inhibition of the PI3K/mTOR pathway

represents a rational therapeutic strategy. Chondrosarcomas with *NRAS* mutations may benefit from treatment with MEK inhibitors.

Introduction

Chondrosarcomas, mesenchymal tumors with cartilaginous differentiation, are biologically and clinically heterogeneous. Complete surgical resection of localized disease remains the only known curative treatment. No systemic treatments have been proven to be effective in the metastatic or unresectable setting. Therefore, there is an urgent need to identify therapeutic targets and to develop novel treatment strategies for patients with this disease (1-4).

Deregulated expression and/or function of receptor tyrosine kinases (RTKs) by gene amplification, mutation, or translocation has been found to be important for cancer cell proliferation, survival, motility and invasion, as well as tumor angiogenesis and resistance to chemotherapy (5, 6). Given their pivotal role in tumor initiation and progression, RTKs have become one of the most prominent target families for drug development, and more than ten inhibitors or antagonistic antibodies have been approved for the treatment of cancer (7, 8).

In this study, we used phospho-RTK arrays to simultaneously assess the phosphorylation status of 40+ RTKs in chondrosarcoma cells under conditions of serum depletion. We found that although several RTKs are constitutively activated, this occurs in differing patterns among different human tumor-derived cell lines. Several RTKs were identified as critical mediators of cell growth through the use of small interfering RNAs (siRNAs) and small molecular inhibitors. To seek a therapeutic strategy for chondrosarcoma, we explored the effects of targeting a common downstream signaling pathway of RTKs on cell growth, and found that the dual pan-class I phosphoinositide-3-kinase (PI3K)/mammalian target of rapamycin (mTOR) inhibitor BEZ235 significantly inhibited growth of chondrosarcomas both *in vitro* and *in vivo*. A chondrosarcoma cell line with an *NRAS* mutation was exclusively sensitive to MEK inhibition.

Materials and Methods

Cell lines and Culture Conditions

Human chondrosarcoma cell lines included SW1353 **(**American Type Culture Collection), CS-1 (gift of Dr. Francis J. Hornicek, Massachusetts General Hospital, Boston, MA), JJ012 (gift of Dr. Joel A. Block, Rush University, Chicago, IL), CH-2879 (kindly provided by Prof. Antonio Llombart-Bosch, Valencia University, Spain) and OUMS-27 (kindly provided by Dr. M. Namba, Okayama University Medical School, Japan) (9-12). Cells were cultured in RPMI 1640 supplemented with 10% fetal bovine serum and 1x Penicillin-Streptomycin-Glutamine (10378-016, Invitrogen, Carlsbad, CA) at 37ºC in a humidified incubator with 95% air and

5% CO2. Cell line identity was verified by high-resolution short tandem repeat (STR) profiling with Promega PowerPlex ®1.2 system.

Phospho-RTK Array

First-generation phospho-RTK arrays (#ARY001, R&D Systems, Minneapolis, MN) were used for assessing the phosphorylation status of 42 RTKs in chondrosarcoma cells under serum-depleted condition. Phospho-RTK analyses were performed as recommended by the manufacturer. Subconfluent cells were washed once with serum-free media, and incubated in serum-depleted medium for 24 hr before harvest. A total of 450 μg of protein was used for the assay.

For qualitative assessment of signal, pixel densities on developed X-ray film were analyzed using a transmission mode scanner and the Adobe Photoshop software. The pixel densities of the areas (49 x 26 pixels, width x height) surrounding the pair of duplicate dots were determined. The pixel density of the PBS negative control was used as a background value and subtracted from each read. RTKs with a signal greater than the positive controls were scored as "+++"; RTKs with a signal level similar to positive controls were scored as "++"; and RTKs with a signal less than positive controls, but 5-fold higher than antibody isotype negative controls were scored as "+". RTKs with signal less than 5-fold higher than the antibody isotype negative control were labeled as "-".

We used second-generation phospho-RTK arrays (#ARY001B, R&D Systems, Minneapolis, MN) to analyze the effects of long-term treatment of BEZ235 on the phosphorylation of RTKs because the first-generation RTK arrays were no longer available. The new arrays include 49 RTK capture antibodies but no longer contain antibody isotype negative controls. The pixel density was measured as described above. The changes in the phosphorylation level of RTKs were determined by comparing the intensity of RTK signals in BEZ235-treated samples to the 0.1% DMSO-treated control samples.

Immunoprecipitation and Immunoblots

Cells were lysed on ice in buffer containing 50 mM HEPES (pH 7.5), 150 mM NaCl, 1 mM EGTA, 10% glycerol, 1% Triton X-100, 100 mM NaF, 10 mM $Na_4P_2O_7 \cdot 10\ H_2O$, 1 mM Na_3VO_4, and 1x Protease Inhibitor Cocktail (Roche Diagnostics, Germany). The following antibodies were used for immunoprecipitation from clarified cell lysates: EGFR (Calbiochem #GR01, San Diego, CA), ERBB2 (Calbiochem #OP15), Insulin Rβ (Santa Cruz #sc-711, Santa Cruz, CA), IGF1Rβ (Santa Cruz #sc-713), EphA2 (Upstate, #05-480), AXL (Santa Cruz #SC-1096), and PDGFRα (Santa Cruz #SC-338). The immunoprecipitants were separated by SDS/PAGE and transferred to nitrocellulose membranes (Bio-Rad, Hercules, CA). Antibodies for immunoblotting were purchased from Calbiochem (ERBB2 #OP15), Lab Vision, Fremont, CA (ERBB3 #MS-201-P), Upstate Biotechnology, Lake Placid, NY (anti-phosphotyrosine antibody 4G10 #05-1050), Sigma, St. Louis, MO (α-tubulin T9026), Santa Cruz (AXL #SC-1096,

PDGFRα #SC-338) and Cell Signaling, Danvers, MA (EGFR #2232, p-EGFR #2234, p-ERBB2 #2243, p-ERBB3 #4791, MET #3127, p-MET #3129, p-PDGFRα #2992, Insulin Rβ #3025, IGF1Rβ #3027, AKT #9272, p-AKT (Ser^{473}) #9271, p-AKT (Thr^{308}) #9275, MAPK #9107, p-MAPK #9101, S6 #2217 and p-S6 ($Ser^{235/236}$) #2211, 4EBP1 #9644, p-4EBP1($Thr^{37/46}$) #2855, p-4EBP1(Ser^{65}) #9451, p-4EBP1 (Thr^{70}) #9455).

Inhibitors
MET inhibitor PHA665752 was purchased from Tocris Biosciences (Ellisville, MO). EGFR/ERBB2 inhibitor BIBW-2992 and MEK inhibitor ARRY-142886 (AZD6244) were purchased from Medicilon (Shanghai, China) and OTAVA (Toronto, Canada), respectively. Insulin-like Growth Factor 1 Receptor (IGF1R)/Insulin Receptor (INSR) inhibitor PQIP was a kind gift from OSI Pharmaceuticals (Melville, NY). PI3K/mTOR inhibitor BEZ235 was purchased from AXON Medchem (Groningen, The Netherlands). PI3K inhibitor GDC-0941 and mTOR inhibitor rapamycin were purchased from Chemdea (Ridgewood, NJ) and Calbiochem, respectively.

siRNA
ON-TARGETplus SMARTpools siRNA against EGFR, ERBB2, ERBB3, MET and a scrambled control were purchased from Dharmacon (Layfayette, CO). Cells were transfected with siRNA at a final concentration of 12.5 or 25 nM with RNAiMAX (Invitrogen) according to the manufacturer's protocol. Cells were incubated with siRNA for 72 or 96 hr prior to analysis of cell viability.

Cell Viability Assays
Cells were plated in 96-well plates at 1000-2000 cells/well in 100 µl of medium containing 10% FBS. After 24 hr, cells were exposed to increasing concentrations of compounds. Each treatment was tested in triplicate. Cell viability was determined after 72 hr using the CellTiter-Glo Luminescent Cell Viability Assay Kit (Promega, Madison, WI) with a modification in the protocol in that the CellTiter-Glo reagent was diluted 1:3 with PBS. The relative luminescence units (RLU) were measured using the FLUOstar Optima plate reader (BMG Labtech GmbH, Germany) and relative cell number was calculated by normalization to the RLU of the control treated cells.

Cell Cycle Analysis
Cells were exposed to inhibitors or 0.1% DMSO for 24 hr and harvested. After washing with ice-cold PBS, cells were fixed in 70% ethanol at 4 ºC for at least 2 hr. Fixed cells were stained in PBS containing 10 µg/mL RNase A and 20 µg/mL propidium iodide (Sigma, St. Louis, MO) in the dark. DNA content analysis was performed by flow cytometry (FACSCalibur; Becton Dickinson, Mountain View, CA) with CellQuest and ModFIT LT software (Becton Dickinson).

Mutation analysis
Genomic DNA was extracted from chondrosarcoma cell lines using DNeasy Blood & Tissue Kit (Qiagen, Valencia, CA) according to the manufacturer's protocol. The coding sequences of selected genes in the PI3K/mTOR and RAS/MAPK pathways were amplified from genomic DNA by PCR with primers listed in the Table 8.1. PCR was performed in 50 µl reactions containing Platinum PCR SuperMix (Invitrogen), 200 ng DNA, 0.3 µM forward and reverse primers using GeneAmp® PCR System 9700 (Applied Biosystems, Carlsbad, CA). The PCR product was purified using Qiaquick PCR purification Kit (Qiagen), and sequenced using Big Dye Terminator V3.1 chemistry in combination with an Applied Biosystems 3730xl Sequencer.
For chondrosarcoma primary tumor tissues, mutation analysis for *PIK3CA* (13) and *NRAS* was performed using DNA available from 89 chondrosarcomas. Hydrolysis probes assay was used to specifically screen for the *PIK3CA* c.1624G>A (p.E542K), c.1633G>A (p.E545K), and c.3140A>G (p.H1047R) and the *NRAS* c.35G>A (p.G12D), c.183A>T (p.Q61H), c.181C>A (p.Q61K), c.182A>T (p.Q61L), and c.182A>G (p.Q61R) hotspot mutations as described (13). Primer and probe sequences for *NRAS* mutation analysis are provided in Table 8.2.

Tumor Xenografts in Nude Mice
JJ012 cells (1 x 10^6) were suspended in PBS, mixed 1:1 with Matrigel (BD Biosciences), and subcutaneously injected into nude female mice (Nu/Nu, Charles River) in a final volume of 100 µl. Treatment began when tumors reached an average size of approximately 50 mm^3. Mice were randomized into statistically identical cohorts (≥ 6 mice/group). BEZ235 was freshly prepared in 10:90 (v/v) N-methyl pyrrolidone: polyethylene glycol 300 (Fluka #69118 and #81160), as described (14), and was administered daily at 35 mg/kg by oral gavage. Tumor xenografts were measured twice a week by ultrasound imaging (VisualSonic Vevo 770, Toronto, Canada), and animal weight was recorded every 3-4 days. Following drug administration, tumors were harvested and fixed for histologic and immunohistochemical analysis or snap-frozen for immunoblot analysis. All procedures were performed according to protocols approved by the Institutional Animal Care and Use Committee of the Dana-Farber Cancer Institute.

Tumor Xenograft Histology and Immunohistochemistry
Haematoxylin and eosin staining as well as immunohistochemistry were performed on five-micron sections of formalin-fixed paraffin-embedded (FFPE) samples from tumors resected from mice. Tissue sections were deparaffinized, rehydrated, and microwaved in 10 mM citrate buffer (pH 6.0) in a 750 W microwave oven for 15 min. Anti-phospho-S6 ribosomal protein (Ser 240/244) primary antibody (Cell Signaling, #2215) was added at a dilution of 1:100 and incubated overnight at 4 ℃. Sections were further processed with horseradish peroxidase-conjugated secondary

antibody. The reaction was detected by 3,3-diaminobenzidine and hematoxylin staining. Images were taken by using Olympus CX41 microscope with QCapture software (QImaging, Surrey, Canada).

Tissue microarray immunohistochemistry

Tissue microarrays (TMAs) containing 157 conventional chondrosarcomas and 25 dedifferentiated chondrosarcomas were described previously (15, 16). All specimens were handled according to the ethical guidelines described in "Code for Proper Secondary Use of Human Tissue in The Netherlands" of the Dutch Federation of Medical Scientific Societies. TMAs contained 2 mm cores of all samples in triplicate. After de-waxing and rehydrating, TMAs were permeabilized with Tris-buffered saline (TBS)/0.5% Tween20 for 30 min at room temperature (RT) and washed several times in distilled water. For antigen de-masking, slides were immersed in citrate buffer (pH 6.0) and antigen retrieval was performed in a pressure cooker (Biocare Medical, UK) for 2 min at 125 °C followed by 10 min at 85 °C. Non-specific binding was blocked in TBS/Tween20 (0.5%) and 10% goat serum for 1 hour at RT. Primary rabbit anti-pS6 antibodies (1:100, New England Biolabs, UK #4857) were incubated with the slides in a humidified chamber at 4 °C over night. After washing 3 times, a secondary goat anti-rabbit Alexa 594 antibody (1:300, Invitrogen, UK) was added. Nuclei were labeled with DAPI and slides were mounted with Prolong Gold Antifade (Invitrogen, UK). Images were acquired with an Olympus Fluoview FV1000 confocal microscope and a 60x oil objective (NA: 1.35). Each image had a size of 2048 x 2048 pixels, a horizontal and vertical dimension of 211 µm x 211 µm and a thickness of 1.292 µm.

Statistical Analysis

Drug concentrations required to inhibit cell growth by 50% (IC_{50}) were calculated by dose-response curve fitting with Prism version 5.0 (GraphPad Software). Comparisons between groups were made using the unpaired *t*-test. Differences in means ± SEM with $p < 0.05$ were considered statistically significant.

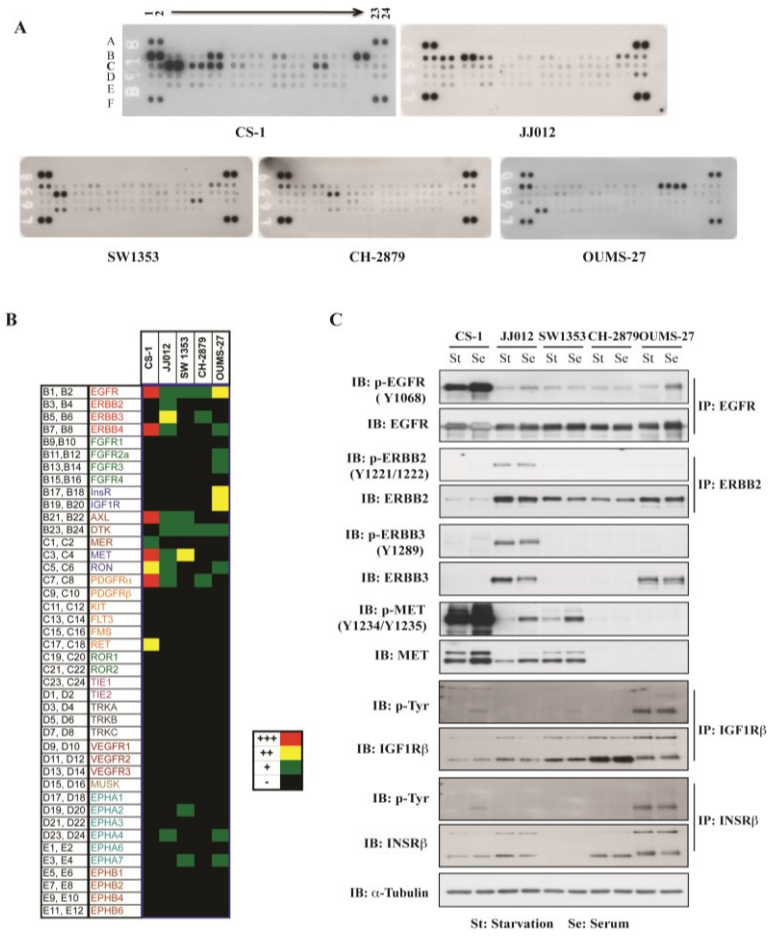

Figure 8.1. Activation of multiple RTKs in chondrosarcoma cells.
A. The phosphorylation status of 42 RTKs in chondrosarcoma cells under serum-depleted conditions was assessed by phospho-RTK arrays. Anti-RTK antibodies spotted on nitrocellulose membrane in duplicate were incubated with cell lysates followed by secondary anti-phosphotyrosine antibody detection. Positive controls are represented in the 4 corners of each blot; negative antibody isotype controls and PBS control are represented in E13-20 and E21-22, respectively. The location and names of capture antibodies are listed in the first and second column of B. **B**. Qualitative heat-blot map of RTK array data. "+++": RTK signal is higher than postive controls; "++": signal is similar to positive controls; "+": signal is lower than postive control but 5-fold higher than antibody isotype negative controls; "-": low signal. **C**. Validation of phospho-RTK array data by immunoblot (IB) or immunoprecipitation (IP)/IB analysis.

Table 8.1. Oligos for gene mutation detection

Gene Symbol	Coding Exon Number	Hotspot Mutation at This Exon§		Primer for Amplification§§ (5'-3')	References	Sequencing Primer 1§§ (5'-3')	Sequencing Primer 2§§ (5'-3')	References
PIK3CA	9	E542, E545	**F**	GATTGGTTCTTTCCTGTCTCTG	1	TTGCTTTTTCTGTAAATCATCTGTG		6
			R	CCACAAATATCAATTTACAACCATTG				
PIK3CA	20	H1047	**F**	TGGGGTAAAGGGAATCAAAAG	1	TGACATTTGAGCAAAGACCTG		6
			R	CCTATGCAATCGGTCTTTGC				
AKT1	2	E17	**F**	M13-CCTAAGAAACAGCTCCCGTACC	2	M13		2
			R	AGCCAGTGCTTGTTGCTTG				
PTEN	5	A130	**F**	TGCAACATTTCTAAAGTTACCTACTTG	2	M13		2
			R	M13-TTTACTTGTCAATTACACCTCAATAAA				
HRAS	2	G12, G13	**F**	CAGGAGACCCTGTAGGAGGA	3	CGCCAGGCTCACCTCTAT	GCGATGACGGAATATAAGCTG	6
			R	CCTATCCTGGCTGTGTCCTG				
HRAS	3	Q61	**F**	AGAGGCTGGCTGTGTGAACT	3	ATGGCAAACACACACAGGAA	GTCCCTGAGCCCTGTCCT	6
			R	TCACGGGGTTCACCTGTACT				
KRAS	2	G12, G13	**F**	TACTGGTGGAGTATTTGATAGT	4	GGTGGAGTATTTGATAGTGTATTAACC	AGAATGGTCCTGCACCAGTAA	6
			R	CATGAAAATGGTCAGAGAAACC				
KRAS	3	Q61	**F**	TTGAAGTAAAAGGTGCACTGT	5	TGCACTGTAATAATCCAGACTGTG	GCATGGCATTAGCAAAGACTC	6,5
			R	GCATGGCATTAGCAAAGACTC				
NRAS	2	G12, G13	**F**	GAACCAAATGGAAGGTCACA	3	GAACCAAATGGAAGGTCACA		3
			R	TGGGTAAAGATGATCCGACA				
NRAS	3	Q61	**F**	TGCCCCCTTACCCTCCACA	4	CACCCCCAGGATTCTTACAG	CCTCATTTCCCCATAAAGATTCAGA	6,4
			R	CCTCATTTCCCCATAAAGATTCA				

				GA			
BRAF	15	V600	**F**	TCATAATGCTTGCTCTGATAGGA	3	TGCTTGCTCTGATAGGAAAATG	6
			R	GGCCAAAAATTTAATCAGTGGA			

[§§]M13 denotes the universal sequencing primer 5'-GTAAAACGACGGCCAGT-3'.

References

1. Samuels Y, et al, Science. 2004. 304(5670):554
2. Parsons DW, et al; Science. 2008 Sep 26;321(5897):1807-12
3. Davies H, et al, Nature. 2002. 417(6892): 949-954
4. Case M, et al, Cancer Research, 2008. 68(16):6803-09
5. Bezieau S, et al.Hum Mutat. 2001.18(3):212-24.
6. Primer3 Plus software at http://www.primer3plus.com

Table 8.2. Primers and reporters for NRAS mutation analysis

Forward Primer Name	Forward Primer Seq.	Reverse Primer Name	Reverse Primer Seq.
NRAS35GA_F	ATGACTGAGTACAAACTGGTGGTG	NRAS35GA_R	GGATTGTCAGTGCGCTTTTCC
NRAS181CA_F	GGTGAAACCTGTTTGTTGGACATAC	NRAS181CA_R	CCTGTCCTCATGTATTGGTCTCTCA
NRAS182AT_F	GGTGAAACCTGTTTGTTGGACATAC	NRAS182AT_R	GTATTGGTCTCTCATGGCACTGTAC
NRAS182AG_F	GGTGAAACCTGTTTGTTGGACATAC	NRAS182AG_R	TGGTCTCTCATGGCACTGTACT
NRAS183AT_F	GGTGAAACCTGTTTGTTGGACATAC	NRAS183AT_R	CCTGTCCTCATGTATTGGTCTCTCA

Reporter 1 Name	Reporter 1 Dye	Reporter 1 Sequence	Reporter 1 Conc.
NRAS35GA_V	VIC	TTGGAGCAGGTGGTGTT	8
NRAS181CA_V	VIC	CTGTACTCTTCTTGTCCAGC	8
NRAS182AT_V	VIC	CAGCTGGACAAGAAGA	8
NRAS182AG_V	VIC	ACAGCTGGACAAGAAG	8
NRAS183AT_V	VIC	CACTGTACTCTTCTTGTCCAG	8

Reporter 2 Name	Reporter 2 Dye	Reporter 2 Sequence	Reporter 2 Conc.
NRAS35GA_M	FAM	TTGGAGCAGATGGTGTT	8
NRAS181CA_M	FAM	CTGTACTCTTCTTTTCCAGC	8
NRAS182AT_M	FAM	ATACAGCTGGACTAGAAGA	8
NRAS182AG_M	FAM	ACAGCTGGACGAGAAG	8
NRAS183AT_M	FAM	ACTGTACTCTTCATGTCCAG	8

Results

Coactivation of RTKs in Chondrosarcoma Cells

We employed phospho-RTK arrays to detect the phosphorylation status of 42 RTKs in five human tumor-derived chondrosarcoma cell lines, and we observed that multiple RTKs were phosphorylated in cells under serum depletion conditions (Fig. 8.1A and B). For example, EGFR, MET, ERBB4, AXL, PDGFRα, RON, and RET were phosphorylated in CS-1 cells. All four EGFR family members were phosphorylated in JJ012 cells. IGF1R, INSR, EGFR and EphA7 were phosphorylated in OUMS-27 cells.

To further validate the phospho-RTK array data, we analyzed by immunoblot the expression and phosphorylation status of the 9 RTKs which were most strongly phosphorylated in the respective chondrosarcoma cell lines. As shown in Fig. 8.1C and Fig. 8.2A, the phospho-RTK array data were confirmed: EGFR (site Tyr^{1068}) was highly phosphorylated in CS-1 cells and less so in the four other cell lines; ERBB2 (site $Tyr^{1221/1222}$) and ERBB3 (site Tyr^{1289}) were highly phosphorylated in JJ012 cells; phosphorylation of MET was detected in CS-1, JJ012, and SW1353 cells, with the highest level in CS-1 cells; INSR β and IGF1Rβ were highly phosphorylated in OUMS-27 cells; the highest phosphorylation level of AXL and EphA2 was observed in CS-1 and SW1353 cells, respectively; and phosphorylation of PDGFRα was detected in CS-1 and CH-2879 cells.

Moreover, most kinases remained constitutively phosphorylated under conditions of serum depletion at levels similar to that seen in the serum-containing media (Fig. 8.1C). While the precise mechanism(s) of kinase activation remains unknown, it appears to be cell-autonomous and independent of exogenous growth factors.

Taken together, the immunoblot data confirmed that RTKs are constitutively activated in chondrosarcoma cells, and that the patterns of activation vary among cell lines.

Effects of RTK inhibition on the Growth of Chondrosarcoma Cells

To explore the involvement of the above-noted highly activated RTKs on the growth and survival of chondrosarcoma cells, we applied small molecule inhibitors and/or siRNAs targeting corresponding RTKs to cells (Fig. 8.3). We examined the effects of the MET inhibitor PHA665752 (17) on MET signaling pathways and cell growth in the CS-1 cell line because of its high level of constitutive phosphorylation. MET phosphorylation at key residues in the kinase domain ($Tyr^{1234/1235}$) was greatly suppressed by treatment with 200 nM PHA665752 in the presence of serum (Fig. 8.3A, left panel). Correspondingly, PHA665752 induced a dramatic reduction in cell number with 43% inhibition at 125 nM (Fig. 8.3B, left panel). We also applied MET siRNAs to exclude the possibility of off-target effects of the small molecule inhibitor. As shown in 8.2B, the expression of MET was dramatically decreased by MET siRNA. Cells transfected with MET siRNA had an obvious decrease (approximately 30%) in cell viability in comparison to control siRNA transfected cells after 72 hr (Fig. 8.2C). These results demonstrate

that MET is involved in the regulation of CS-1 chondrosarcoma cell growth. There was no significant effect of MET pathway inhibition in cell lines JJ012 and SW1353 that have low basal phospho-MET levels (Fig. 3B, left panel). In addition, we determined the effects of the EGFR inhibitor gefitinib and the anti-EGFR antibody cetuximab on the viability of CS-1 cells because of the high phosphorylation level of EGFR, but no significant changes were observed (data not shown).

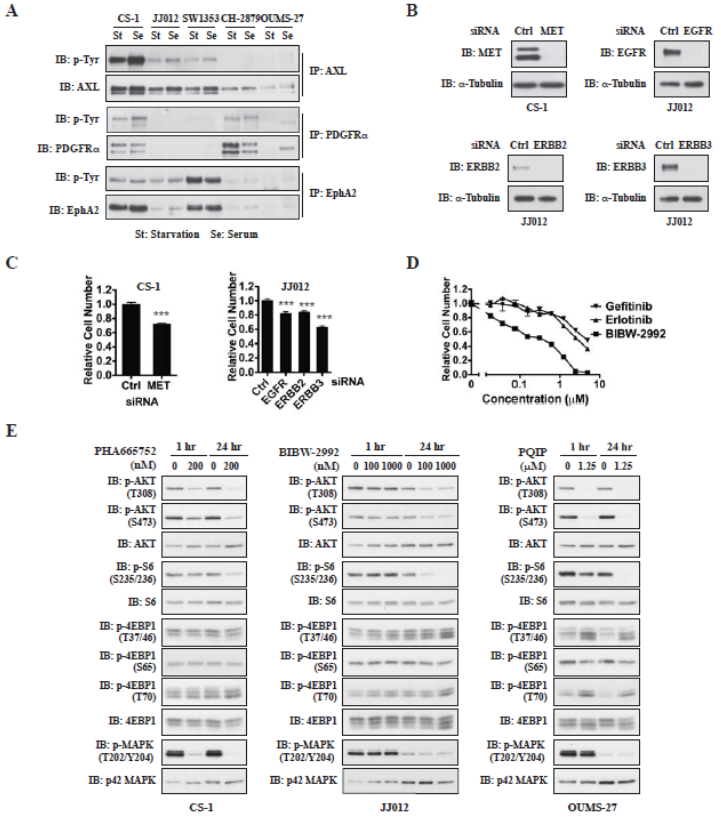

Figure 8.2. Effects of RTK inhibition in chondrosarcoma cells.

A. Validation of phospho-RTK array data by immunoblot (IB) or immunoprecipitation (IP)/IB analysis. B. siRNA-mediated knockdown of RTK expression at 48 hr. C. siRNA-mediated knockdown of RTKs on growth of CS-1 (at 72 hr) and JJ012 (at 96 hr) cells evaluated by CellTiter-Glo viability assay. Values represent mean ± SEM (n>3). ***, $P<0.001$, compared with scrambled siRNA-transfected cells. D. Effects of EGFR kinase family inhibitors on cell viability of JJ012 cells were evaluated by CellTiter-Glo viability assay at 72 hr. E. Effects of RTK inhibition on the signaling of PI3K/mTOR and MAPK pathways were evaluated by immunoblots.

In JJ012 cells, four members of the EGFR kinase family were phosphorylated. The irreversible EGFR/ERBB2 inhibitor BIBW-2992 (18) decreased phosphorylation of ERBB2 and ERBB3 (Fig. 8.3A, central panel), and inhibited cell growth in a dose-dependent manner with an IC_{50} of 0.38 ± 0.02 μM (Fig. 8.3B, central panel). siRNA-mediated knockdown of ERBB3 also significantly reduced cell number (37.7% ± 6.1%) compared to control siRNA at 96 hr after transfection (P<0.001; Fig. 8.2B and 8.2C). However, the EGFR-specific inhibitors gefitinib and erlotinib only demonstrated mild effects as did siRNA mediated knockdown of EGFR and ERBB2 (Fig. 8.2C and 8.2D). These findings suggest that EGFR family kinases, and in particular ERBB3, are important regulators of the growth of JJ012 cells.
In OUMS-27 cells, IGF1R and INSR are highly phosphorylated. Treatment with the IGF1R/INSR inhibitor PQIP (19, 20) decreased phosphorylation of IGF1Rβ and INSRβ (Fig. 8.3A, right panel), and inhibited growth in a dose-dependent manner with an IC_{50} of 1.42 ± 0.08 μM (Fig. 8.3B, right panel). These data suggest that the insulin receptor kinase family is involved in the growth of OUMS-27 cells.

Effects of RTK Inhibition on the Activity of PI3K/mTOR and MAPK Pathways in Chondrosarcoma cells

We further examined the effects of RTK inhibition on the PI3K/mTOR and MAPK pathways. In MET-dependent CS-1 cells, treatment with the MET inhibitor PHA665752 for 2 hr led to a dose-dependent decrease in the phosphorylation of AKT at Thr^{308} and Ser^{473}, S6 at $Ser^{235/236}$ and p44/42 MAPK at Thr^{202}/Tyr^{204} (Fig. 8.3A, left panel). In JJ012 cells, phosphorylation of AKT and S6 was partially reduced by BIBW-2992 treatment, but no effect on MAPK phosphorylation was observed (Fig. 8.3A, central panel). In OUMS-27 cells, IGF1R/INSR inhibitor PQIP treatment decreased AKT and S6 phosphorylation in a dose-dependent manner, with complete inhibition at 1.25 μM, but had no effect on MAPK phosphorylation (Fig. 8.3A, right panel). The inhibition of phosphorylation in the presence of the above inhibitors was continued for at least 24 hr, with the level of phosphorylation at 24 hr even somewhat lower (Fig. 8.2E). No significant inhibition on the phosphorylation of 4EBP1 was observed following the treatment of RTK inhibitors for 1 or 24 hr (Fig. 8.2E).

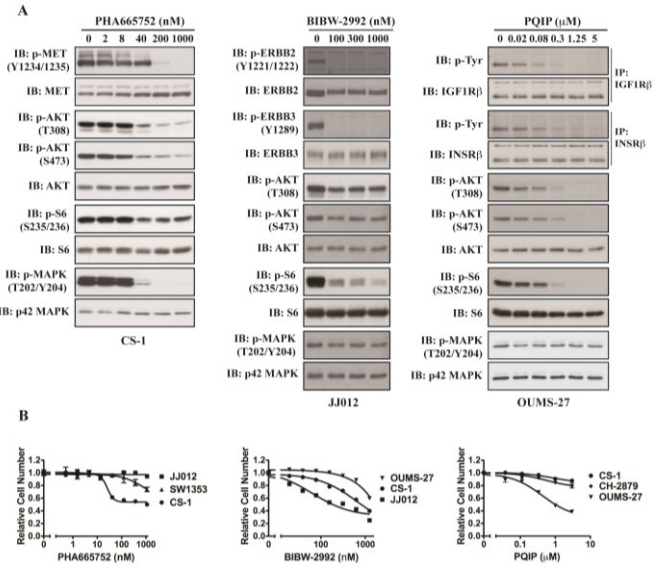

Figure 8.3. Effects of RTK inhibition in chondrosarcoma cells. **A.** Effects of MET inhibitor PHA665752 (left panel, at 2 hr), EGFR/ERBB2 inhibitor BIBW-2992 (central panel, at 2 h) and IGF1R/INSR inhibitor PQIP (right panel, at 6 h) on the phosphrylation of RTKs and their downstream effectors were evaluated by immunoblot. **B.** Effects of RTK inhibitors on cell viability were evaluated by CellTiter-Glo assay at 72 hr.

Chondrosarcomas have PI3K/mTOR Activation and are Sensitive to Inhibitors in vitro

The above data suggest that RTKs are important mediators of chondrosarcoma cell growth. However, the heterogeneity of implicated pathways poses a considerable challenge to the clinical evaluation of any single tyrosine kinase inhibitor for the treatment of this disease. Targeting common pathways downstream of RTKs may instead be a method to inhibit cell growth irrespective of the particular upstream signaling molecule.

We hypothesized that the PI3K/mTOR pathway might commonly mediate signaling from heterogeneous RTK activation and thus we examined the activity of this pathway in human primary chondrosarcoma tissue specimens. As an established surrogate of PI3K/mTOR pathway activity, we analyzed the S6 phosphorylation status in chondrosarcoma tissue microarray samples by immunohistochemical staining. In total, 73 out of 106 (69%) conventional chondrosarcomas and 11 out of 25 (44%) dedifferentiated chondrosarcomas were positive (Table 8.3, Fig. 8.4).

In order to determine whether PI3K/mTOR signaling and S6 phosphorylation were relevant to chondrosarcoma growth, we tested the effects of BEZ235, a dual PI3K/mTOR inhibitor (14). Treatment with BEZ235 potently inhibited the growth of all of the chondrosarcoma cell lines, with IC_{50} values below 10 nM (Fig. 8.8A, left panel). Cell cycle analysis showed a substantial increase in the proportion of cells in the G_0/G_1 phase of the cell cycle after treatment with the inhibitor (Fig. 8.5A). No induction of apoptosis was observed (data not shown).

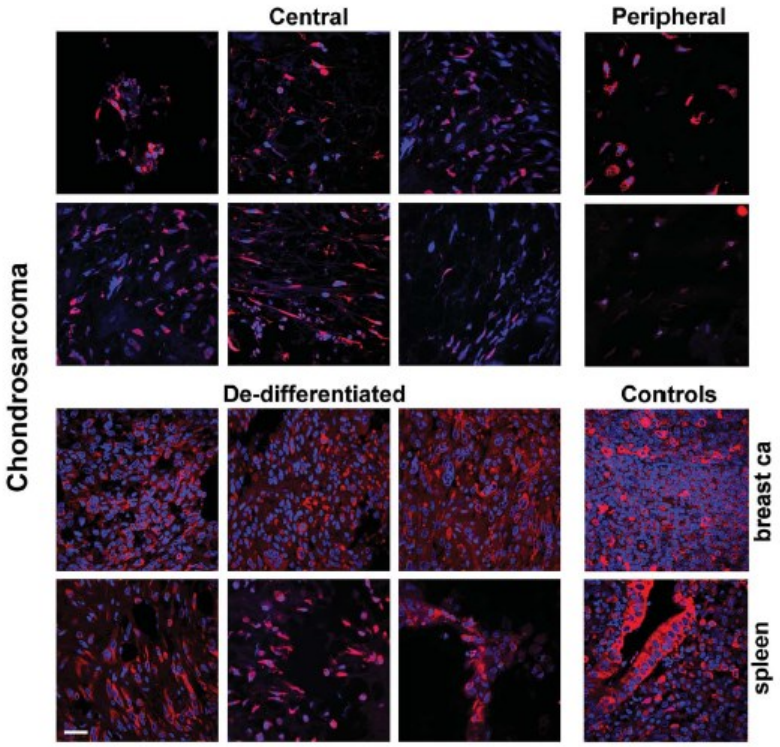

Figure 8.4. S6 phosphorylation in chondrosarcoma clinical tissue microarray samples. Confocal images of immune-labeled sections with DAPI and anti-pS6 antibody in chondrosarcoma samples. Example images from central chondrosarcoma, peripheral chondrosarcoma and high grade areas of dedifferentiated chondrosarcoma display the sometimes sparse distribution and heterogeneity of cellular labeling in tumor regions. Positive controls are of breast carcinoma and normal spleen. Bar 20μm.

We also tested the effects of the PI3K inhibitor GDC-0941 and the mTOR inhibitor rapamycin on cell growth. Each were significantly less potent than BEZ235, with GDC-0941 inhibiting the growth of chondrosarcoma cell lines with IC_{50} values of 0.9-2.5 μM, and rapamycin causing 22-49% growth inhibition at a concentration of 1000 nM (Fig. 8.5B).

Functionally important mutations in the PI3K/mTOR pathway have been reported as potential predictors of sensitivity to the treatment of PI3K/mTOR pathway inhibitors (21, 22). We sequenced selected hotspot sites, including *PIK3CA* (exon 9 and 20), *AKT1* (exon 2), and *PTEN* (exon 5). However, no mutations were detected in these five chondrosarcoma cell lines (data not shown). Moreover, *PIK3CA* hotspot mutations were absent in all 88 chondrosarcomas tested using hydrolysis probe assays (data not shown).

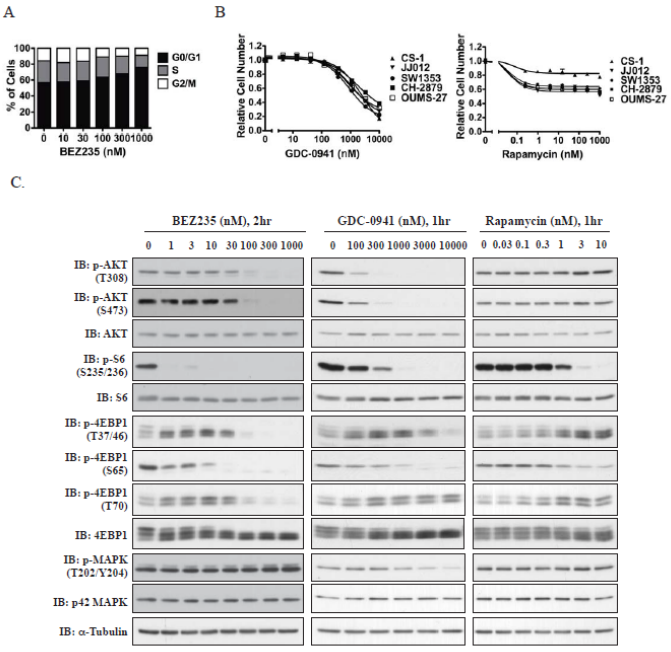

Figure 8.5. Effects of PI3K/mTOR pathway inhibitors in chondrosarcoma cells. A. Cell cycle analysis of JJ012 cells following 24hrs treatment with BEZ235. B. Effects of PI3K inhibitor GDC-0941 and mTOR inhibitor rapamycin on chondrosarcoma cell viability evaluated by CellTiter-Glo assay after 72 hr. Values represent mean ± SEM (n=3). C. Effects of BEZ235, GDC-0941 and rapamycin treatment on the phosphorylation of AKT, S6, 4EBP1, and MAPK in JJ012 cells were evaluated by immunoblot.

Sustained suppression of phosphorylation of S6 and 4EBP1, and feedback induction of AKT phosphorylation after prolonged treatment with BEZ235 in vitro

We used the phosphorylation state of AKT, S6 [a major substrate of p70 S6 kinase 1 (S6K1)], and 4EBP1 as markers to monitor the activity of PI3K/mTOR pathway inhibitors. The Thr^{308} site and Ser^{473} sites of AKT are regulated by PDK1 (a major downstream effector of PI3K kinase) and the mTORC2 complex, respectively. The mTORC1 complex catalyzes the phosphorylation of S6K1 and 4EBP1. (23-25) Following 2 hr treatment of JJ012 with BEZ235, the phosphorylation of S6 and the Ser^{65} site of 4EBP1 were suppressed at 1 nM and 30 nM, respectively, and the phosphorylation of AKT and the $Thr^{37/46}$ and Thr^{70} sites of 4EBP1 was inhibited at 100 nM (Fig. 8.5C). Following 24 hr treatment, the inhibition of S6 and 4EBP1 phosphorylation was well sustained or even strengthened (Fig. 8.8B, left panel), while the initial inhibition on the AKT phosphorylation was dramatically reversed at 24 hr with an increase in phosphorylation level at the Thr^{308} site of AKT at 10 and 100 nM. At 300 nM, BEZ235 treatment still potently inhibited the phosphorylation of Ser^{473} at 24 h, keeping AKT activity in a partially suppressed status, as phosphorylation of both Thr^{308} and Ser^{473} sites is required for full AKT activation (26, 27) (Fig. 8.8B, left panel). We further examined the effects of

BEZ235 treatment on the PI3K/mTOR signaling in the other four chondrosarcoma cell lines, and similar results were observed: the phosphorylation of S6, 4EBP1 and the Ser^{473} site of AKT, but not Thr^{308} site, were effectively inhibited by 300 nM BEZ235 treatment at 24 hr (Fig. 8.6A-8.6D). The effects of BEZ235 on MAPK phosphorylation were also examined, and a slight increase in its phosphorylation level was observed when JJ012 and SW1353 cells were treated with 100-1000 nM BEZ235 (Fig. 8.5B, Fig. 8.6B).

In comparison to BEZ235, GDC-0941 effectively inhibited the phosphorylation of AKT at 300 nM, but required a much higher concentration (1000-10000 nM) to inhibit the phosphorylation of S6 and 4EBP1 (Fig. 8.5C). Following 24 h treatment with GDC-0941, the phosphorylation level of the Thr^{308} site of AKT remained suppressed. A slight induction of the phosphorylation signal of S6 and Ser^{473} site of AKT was observed in OUMS-27 and CS-1 cells, respectively (Fig. 8.6A and 8.6D).

Rapamycin treatment blocked S6 phosphorylation but only slightly decreased the phosphorylation of 4EBP1 at 10 nM (Fig. 8.5C, Fig. 8.8B). It has previously been demonstrated that mTORC1 inhibition can lead to feedback activation of PI3K in cancer cells (25). In SW1353 and OUMS-27 cells, we also observed a dramatic and lasting increase in the phosphorylation level of AKT at Thr^{308} and Ser^{473} following rapamycin treatment (Fig. 8.6B and 8.6D). However, in JJ012 cells rapamycin treatment enhanced the phosphorylation level of AKT only at Thr^{308}, and not at Ser^{473} (Fig. 8.8B). There were no obvious changes observed in CS-1 and CH-2879 cells (Fig. 8.6A and 8.6C).

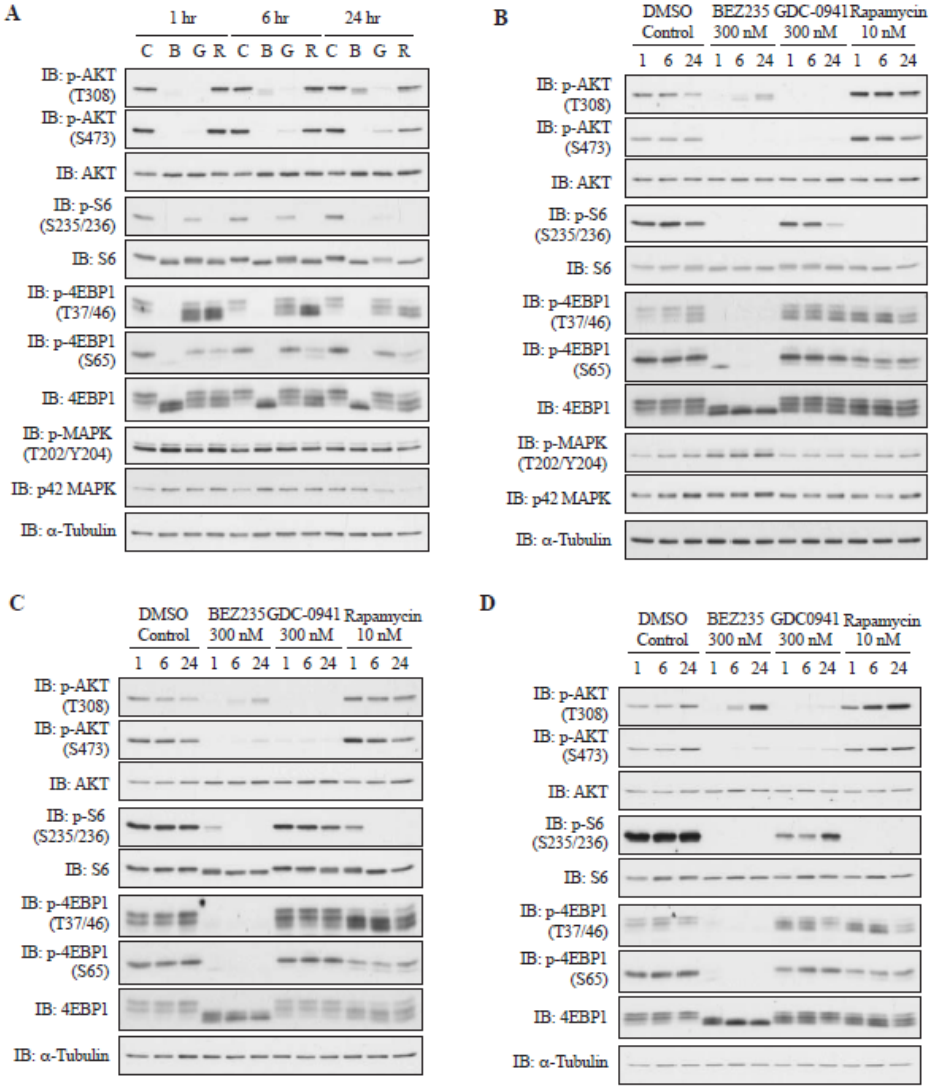

Figure 8.6. Time-dependent effects of PI3K/mTOR pathway inhibitors on the activation of AKT and MAPK signaling pathway in chondrosarcoma cells.
A. Effects of BEZ235 (B), GDC-0941 (G), rapamycin (R), and DMSO control (C) on the phosphorylation of AKT, S6, 4EBP1, and MAPK in CS-1 (panel **A**), SW1353 (panel **B**), CH-2879 (panel **C**), and OUMS27 (panel **D**). Cells were evaluared by immunoblot at 1, 6, and 24 hr.

Table 8.3. Phosphorylated S6 Staining in Chondrosarcoma Clinical Samples

	Total	Number Positive for pS6[§] (%)
Enchondroma	7	5 (71)
Osteochondroma	6	5 (83)
Conventional Chondrosarcoma	106	73 (69)
Central Chondrosarcoma	80	58 (73)
Grade I	37	27 (73)
Grade II	30	20 (67)
Grade III	13	11 (85)
Peripheral Chondrosarcoma	26	15 (58)
Grade I	14	9 (64)
Grade II	9	5 (56)
Grade III	3	1 (33)
Dedifferentiated Chondrosarcoma	25	11 (44)

[§] pS6: phosphorylated S6 staining as performed on tissue microarrays

In vivo effects of PI3K/mTOR inhibitor BEZ235 on chondrosarcoma tumor growth and PI3K/mTOR signaling

The antitumor activity of BEZ235 was studied in a mouse xenograft model of the JJ012 cell line treated for 21 days with drug or vehicle control. As shown in Fig. 8.7A, BEZ235 significantly suppressed tumor growth ($p<0.01$). No significant weight loss of the mice was observed (data not shown). Histologic analysis demonstrated a marked decrease in tumor cell viability as well as in the phosphorylation of S6 protein (Fig. 8.7B). We also explored the effects of short-term (2 hr) and long-term (21 days+2 hr) treatment of BEZ235 on PI3K/mTOR signaling in JJ012 xenografts by immunoblots (Fig. 8.7C). The phosphorylation signal of S6 was diminished in all of the xenografts samples treated with 35 mg/kg BEZ235. The multiple phosphorylation sites of 4EBP1 were differentially dephosphorylated: phosphorylation of Ser^{65} site was suppressed, and phosphorylation of Thr^{70} and $Thr^{37/46}$ sites were partially decreased, which may enable 4EBP1 to partially block the function of the eukaryotic translation initiation factor 4E (eIF4E), since the phosphorylation of Thr^{70} and Ser^{65} sites are critical for the release of 4E-BP1 from eIF4E (28, 29). BEZ235 treatment also decreased the phosphorylation of AKT at the Ser^{473} site, but the inhibition became less profound following the prolonged treatment of BEZ235. A slight increase in phosphorylation of Thr^{308} of AKT was observed.

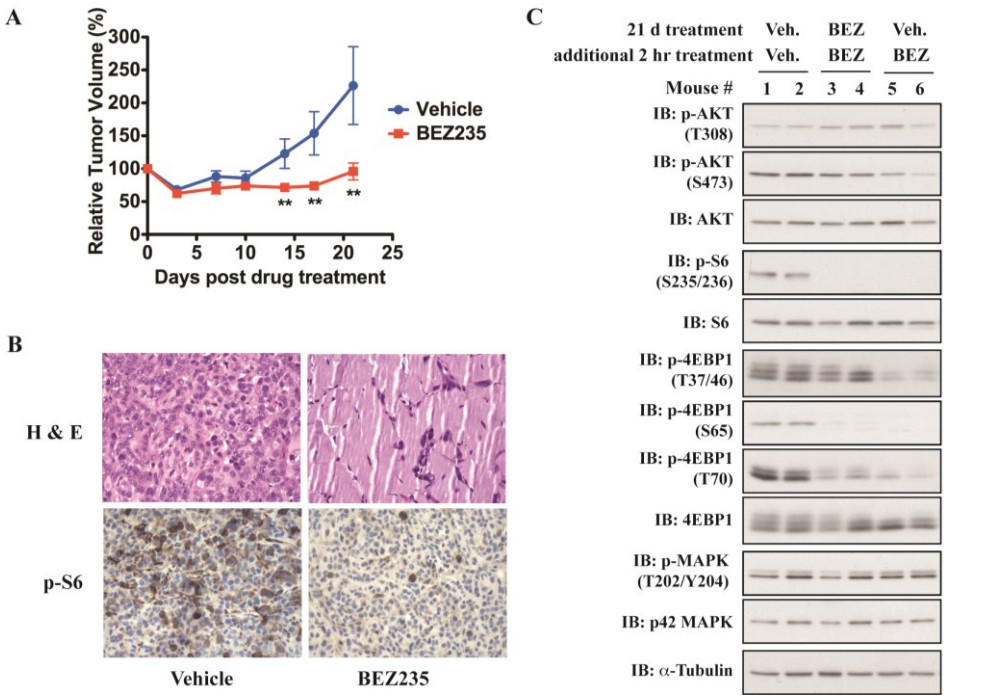

Figure 8.7. BEZ235 inhibits *in vivo* growth of JJ012 chondrosarcoma xenografts and reduced phosphorylation of S6 and 4EBP1

A. JJ012 xenografts were treated with 35 mg/kg BEZ235 daily or with vehicle alone by oral gavage for 21 days. Tumor size was determined by ultrasound every 3-4 days. Values represent mean volume ± SEM (n>5). **, $p<0.01$, compared with respective control group treated with vehicle. **B**. Representative examples of hematoxylin and eosin staining in tumor xenografts 21 days after vehicle or BEZ235 treatment; and representative immunohistochemistry staining for phospho-S6 in tumor xenografts 2 hr after vehicle or BEZ235 treatment. Original magnification: 400×. **C**. After 21 days of BEZ235 (BEZ) or vehicle (Veh.) treatment, 6 mice were given an additional dose of vehicle or 35 mg/kg BEZ235 2 hr before the tumors were harvested. The phosphorylation levels of AKT, S6, 4EBP1, and MAPK in those xenograft tumors were examined by immunoblots.

BEZ235-induced hyperphosphorylation of IGF1R family kinases and feedback activation of AKT in chondrosarcoma cells

Since it has been reported that rapamycin can induce feedback activation of AKT through RTK-dependent mechanisms (25), we used RTK arrays to explore the changes in RTK phosphorylation following 24 hr treatment with BEZ235. A common increase in the phosphorylation levels of IGF-1R and/or INSR was observed (Fig. 8.8C and 8.9A and 8.9B). We further checked the combinational effects of BEZ235 and the IGF1R/INSR inhibitor PQIP on AKT phosphorylation at the Thr^{308} site in OUMS-27 and SW1353 cells, and found that this remained suppressed following combination treatment with BEZ235 and PQIP for 24 hr (Fig.

8.8D). These data suggest that BEZ235 induces feedback activation of IGF1R/INSR, which further induces AKT phosphorylation in chondrosarcoma cells.

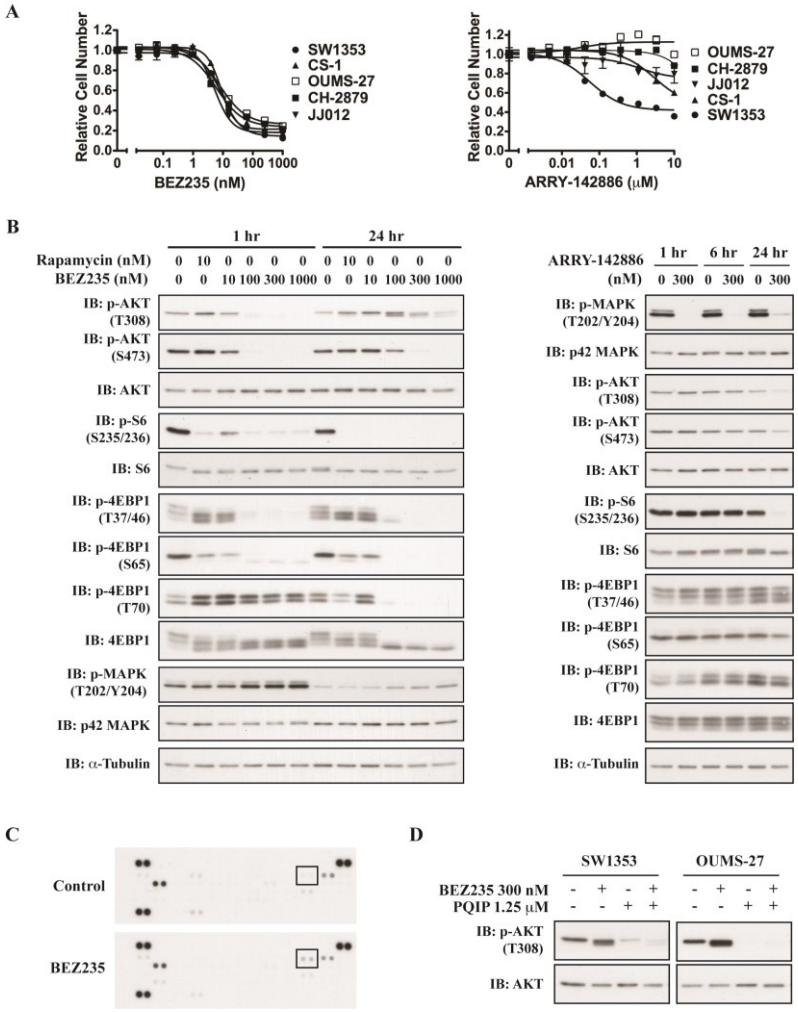

Figure 8.8. Effects of PI3K/mTOR inhibitor BEZ235 and MEK Inhibitor ARRY-142886 on chondrosarcoma cells *in vitro*.

A. Dose-dependent reduction in chondrosarcoma cell number following 72 hr treatment with BEZ235 (left panel) or ARRY-142886 (right panel). Values represent mean ± SEM (n=3). **B.** Effects of rapamycin, BEZ235 (left panel, in JJ012 cells), and ARRY-142886 (right panel, in SW1353 cells) treatment on the activation of AKT, S6, 4EBP1, and MAPK. **C**. The phosphorylation status of 49 RTKs in SW1353 cells was assessed by phospho-RTK arrays after 24 hr treatment with 0.1% DMSO (control) or 300 nM BEZ235. The location and names of capture antibodies are listed in Fig. 8.9B. The IGF1R kinase is highlighted with a rectangle. **C**. Combinational treatment with BEZ235 and IGF1R/INSR inhibitor PQIP prevented AKT from reactivation as evaluated by immunoblot at 24 hr.

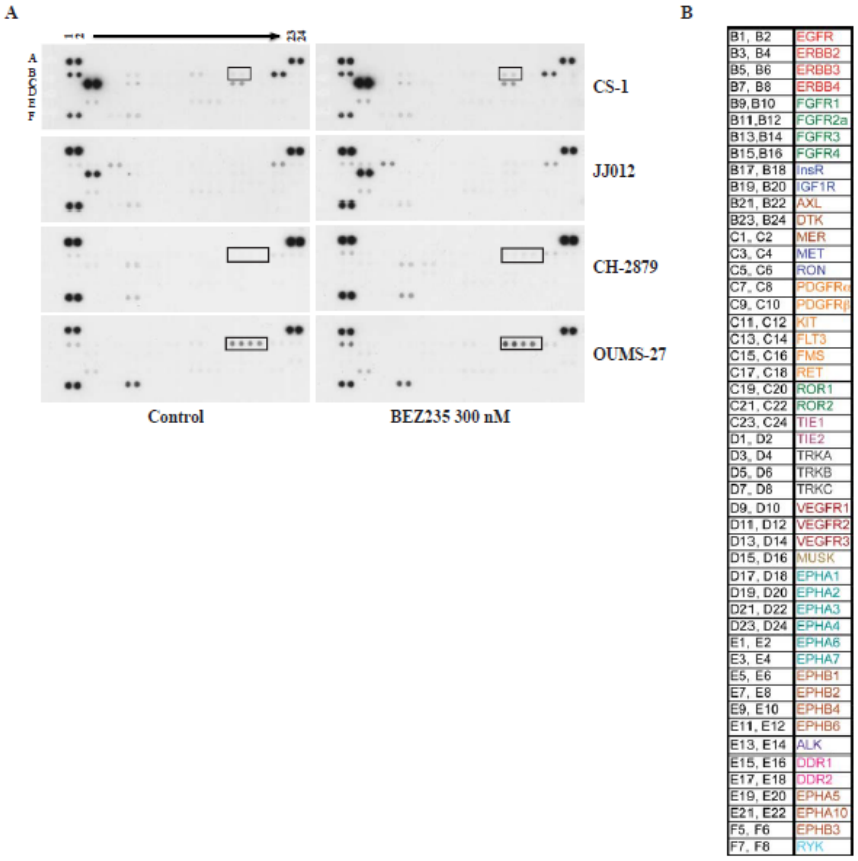

B

B1, B2	EGFR
B3, B4	ERBB2
B5, B6	ERBB3
B7, B8	ERBB4
B9,B10	FGFR1
B11,B12	FGFR2a
B13,B14	FGFR3
B15,B16	FGFR4
B17, B18	InsR
B19, B20	IGF1R
B21, B22	AXL
B23, B24	DTK
C1, C2	MER
C3, C4	MET
C5, C6	RON
C7, C8	PDGFRα
C9, C10	PDGFRβ
C11, C12	KIT
C13, C14	FLT3
C15, C16	FMS
C17, C18	RET
C19, C20	ROR1
C21, C22	ROR2
C23, C24	TIE1
D1, D2	TIE2
D3, D4	TRKA
D5, D6	TRKB
D7, D8	TRKC
D9, D10	VEGFR1
D11, D12	VEGFR2
D13, D14	VEGFR3
D15, D16	MUSK
D17, D18	EPHA1
D19, D20	EPHA2
D21, D22	EPHA3
D23, D24	EPHA4
E1, E2	EPHA6
E3, E4	EPHA7
E5, E6	EPHB1
E7, E8	EPHB2
E9, E10	EPHB4
E11, E12	EPHB6
E13, E14	ALK
E15, E16	DDR1
E17, E18	DDR2
E19, E20	EPHA5
E21, E22	EPHA10
F5, F6	EPHB3
F7, F8	RYK

Figure 8.9. Feedback effects on phosphorylation of RTKs following 24hr treatment of BEZ235 in chondrosarcoma cells.

A. The phosphorylation status of 49 RTKs was assessed by phospho-RTK arrays after 24 hr treatment with 0.1% DMSO (Control) of 300nM BEZ235. The positive controls are represented at A1-2, A23-24, adn F1-2; the PBS negative control is represented at F23-24. The location of capture antibodies for RTKs is listed in panel B. The changes in the phosphorylation level of IGF1R kinase family members were highlighted with a rectangle. **B**. The location of capture antibodies in RTK array.

NRAS-Mutated Chondrosarcoma Cell Line is Sensitive to Inhibition of MAPK pathway

In contrast to BEZ235, the MEK inhibitor ARRY-142886 (30) only inhibited the growth of SW1353, and had minimal effects on the other 4 chondrosarcoma cell lines (Fig. 8.5A, right panel). Sequencing of hotspot mutation-containing exons of *HRAS, KRAS, NRAS* (exon 2 and 3) and *BRAF* (exon 15) genes (31, 32) revealed a heterozygous c.181C>A (Q61K) mutation in *NRAS* in SW1353 cells (Fig. 8.10A). No mutation was found in these exons in the other four cell lines.

We additionally performed hotspot mutation analysis for NRAS exons 2 and 3 in DNA from frozen chondrosarcoma clinical samples. NRAS mutations were found to be specific for a subset of conventional central chondrosarcomas: six samples (12%) harbored NRAS mutations, including 2 c.181C>A (Q61K) mutations, and 4 c.182A>T (Q61H) mutations (Table 8.4). The other chondrosarcoma subtypes were negative.

We examined the effects of ARRY-142886 on the MAPK and PI3K/mTOR pathways in SW1353 cells. Treatment with ARRY-142886 for 1 hr led to a dose-dependent decrease in the phosphorylation of MAPK with complete inhibition at 300 nM, but had no obvious effect on the phosphorylation of AKT, S6, or 4EBP1 (Fig. 8.5B, right panel, Fig. 8.10B). With more prolonged treatment, a dramatic decrease in S6 phosphorylation and a partial inhibition of AKT phosphorylation were observed following 24 hr treatment with ARRY-142886 (Fig. 8.8B, right panel). The mechanism is unclear.

We also examined the combinational effects of BEZ235 and ARRY-142886 on MAPK and AKT signaling pathways in SW1353 cells, and found stronger inhibition in comparison to BEZ235 treatment alone (Fig. 8.10C). Correspondingly, the combination of BEZ235 and ARRY-142886 had additive inhibitory effects on the cell viability in SW1353 cells (Fig. 8.10D). However, apoptosis was not observed following the combination treatment.

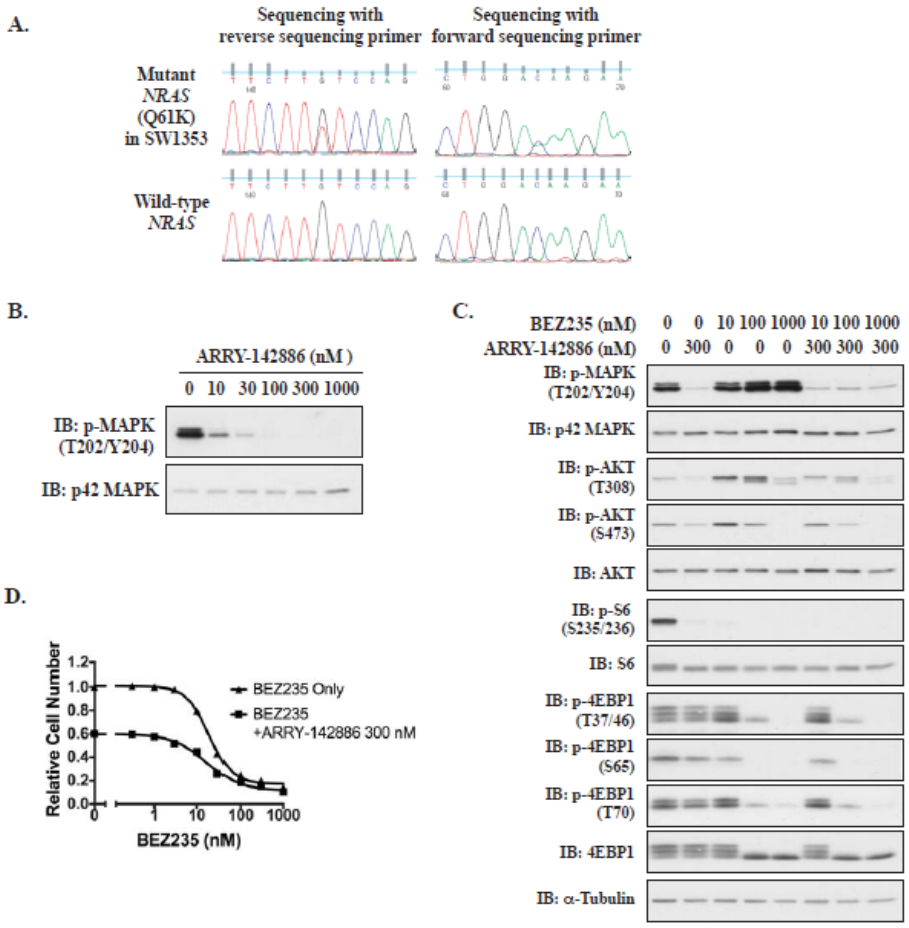

Figure 8.10. Combinational effects of BEZ235 and MEK inhibitor ARRY-142886 in SW1353 cells with *NRAS* mutation.

A. Sequencing was performed with forward or reverse sequencing primer. The top chromatogram is the mutant sequence of *NRAS* in SW1353 cells, and the bottom is a wild-type sequence. **B.** Effects of MEK inhibitor ARRY-142886 on MAPK phosphorylation evaluated by immunoblot at 1hr. **C**. Effects of combination treatment with BEZ235 and ARRY-142886 on the signaling of PI3K/mTOR pathway and MAPK pathway analyzed by immunoblot at 24hr in SW1353 cells. **D**. Effects of combination treatment with BEZ235 and ARRY-142886 on cell viability evaluated by CellTiter-Glo cell viability assay at 72 hr in SW1353 cells.

Discussion

Sarcomas constitute a heterogeneous family of mesenchymal tumors with divergent lineages of differentiation. Some sarcomas have well-defined pathogenic genetic lesions, such as activating kinase mutations in gastrointestinal stromal tumors (GIST) or translocations that yield aberrant chimeric transcription factors in Ewing sarcoma, for example. Many other subtypes of sarcomas have no known dominant molecular pathogenic lesions to explain disease initiation, maintenance, or progression. Chondrosarcomas fall in this latter category (1, 4, 33) although recent reports indicate that approximately half have mutations in *IDH1* or *IDH2* (34), which are considered to be an early event and of which the functional consequences remain to be established. Chondrosarcomas are notoriously resistant to conventional chemotherapeutic agents and currently no effective systemic therapies exist for metastatic or unresectable disease. A better molecular and biochemical understanding of this malignancy may yield novel and effective treatment approaches.

We explored the potential role of receptor tyrosine kinases in driving chondrosarcoma cell survival and proliferation. We identified constitutive, serum-independent activation of the MET, EGFR family, and IGF1R/INSR family kinases in multiple cell lines through as of yet unidentified mechanisms. Inhibition of RTK signaling by treatment with small molecule kinase inhibitors or by suppressing RTK expression with siRNA led to alterations in phosphorylation of downstream pathway members and a concomitant decrease in cellular proliferation. The incomplete block of cell growth suggests that other parallel pathways are also likely to be important.

Consistent with our data demonstrating RTK activation, strong and common phosphorylation of the downstream signaling proteins AKT, MEK, and S6 kinase was previously demonstrated using kinase substrate peptide arrays and extracts from chondrosarcoma cell lines and primary cultures (35). Here, we have linked RTK activation in chondrosarcoma cells to PI3K/AKT/mTOR signaling by demonstrating that RTK inhibitors suppress AKT and S6 phosphorylation. Moreover, high-level phosphorylation of S6 was found in approximately 70% of chondrosarcoma tumors, suggesting that activation of the PI3K/AKT/mTOR pathway in cell lines is clinically relevant. We also identified functional mutations of *NRAS* in a chondrosarcoma cell line and in clinical samples; these may contribute to the activation of the MAPK signaling pathway.

Notably, the heterogeneous pattern of RTK and NRAS activation among the varying human tumor-derived chondrosarcoma cell lines poses a challenge for the potential clinical development of tyrosine kinase inhibitors for this disease. Molecular profiling of signaling pathways in any given individual tumor might suggest a specific kinase inhibitor as a rational agent to test in that specific individual patient. Accordingly, such drugs could be studied in selected groups of patients, but this is a highly personalized and potentially cumbersome approach to

rare tumor subsets. An alternative approach may be to target shared downstream kinases, such as components of the PI3K/mTOR pathway. Indeed, the PI3K/mTOR inhibitor BEZ235 dramatically and potently blocked the growth of all chondrosarcoma cell lines *in vitro* and inhibited tumor growth *in vivo*. These data suggest that PI3K/mTOR pathway inhibitors, many of which are currently in clinical development (36-38), should be studied for their efficacy in the treatment of advanced chondrosarcoma.

In chondrosarcoma cells, BEZ235 exhibited more potent inhibition on cell growth than the mTORC1 inhibitor rapamycin and PI3K inhibitor GDC-0941. A detailed comparison of the effects of these three inhibitors on PI3K/mTOR signaling showed that BEZ235 is a more potent inhibitor of the phosphorylation of S6 and 4EBP1, important regulators of global protein synthesis and cap-dependent protein translation, respectively (39). Increases in the overall rate of protein synthesis as well as enhanced translation of oncogenes are often driven by the hyperactivation of RTKs and their downstream effectors, allowing uncontrolled growth and survival of cancer cells (40). The ability of BEZ235 to inhibit S6 and 4EBP1 phosphorylation both *in vitro* and *in vivo* may account for its potent antitumor activity in chondrosarcoma as well as in other cancer types (41, 42).

In the models presented here, the major effect of BEZ235 treatment was primarily cell cycle inhibition and a delay in tumor growth. A combination of BEZ235 and IGF1R/INSR inhibitor prevented AKT from reactivation, but still failed to induce apoptosis. High expression of BCL2 family members was recently shown to play an important role in chemoresistance of chondrosarcoma, and inhibition of BCL2 was shown to repair the apoptotic machinery, rendering chondrosarcoma cells chemosensitive (43). Inhibition of BCL2 may further supplement the observed outcome of PI3K/mTOR blockade by inducing cell apoptosis.

Recently, growth inhibitory effects of BEZ235 were reported in osteosarcoma, Ewing sarcoma, and rhabdomyosarcoma model systems (44). However, aside from their common mesenchymal origin, these sarcoma subtypes are generally chemosensitive and are unrelated to chemo- and radio-resistant chondrosarcomas, strongly differing in their biology and clinical behavior.

Table 8.4. NRAS Mutation Analysis in Chondrosarcoma Clinical Samples

	Total	Number with NRAS 181 C>A (%)	Number with NRAS 183 A>T (%)	Total number with NRAS mutations (%)
Chondrosarcoma				
Conventional Central	50	2 (4)	4 (8)	6 (12)
Grade I	13	0 (0)	0 (0)	0 (0)
Grade II	28	2 (7.1)	1 (3.6)	3 (10.7)
Grade III	9	0 (0)	3 (33.3)	3 (33.3)
Conventional Peripheral	17	0 (0)	0 (0)	0 (0)
Dedifferentiated Chondrosarcoma	10	0 (0)	0 (0)	0 (0)
Clear Cell Chondrosarcoma	9	0 (0)	0 (0)	0 (0)
Mesenchymal Chondrosarcoma	3	0 (0)	0 (0)	0 (0)

In our study, an activating *NRAS* mutation was identified in 12% of clinical chondrosarcoma samples. Two of these 6 chondrosarcoma samples also contain an *IDH1* R132C mutation (45). Similarly, SW1353 carries *IDH2* (45) and *NRAS* mutations, indicating that these mutations are not mutually exclusive. SW1353 cells were found to be sensitive to MEK inhibitors as well as to a PI3K/mTOR inhibitor. A combination of these two inhibitors had additive suppresion of SW1353 cell viability but did not induce apoptosis, consistent with reported effects of the combination in colorectal carcinomas with RAS mutations (46).

Taken together, our study identifies the heterogeneity of RTK activation present in chondrosarcoma cell lines, and suggests that inhibition of the PI3K/mTOR pathway, a common signaling pathway downstream of RTKs, may be a rational therapeutic strategy for the treatment of advanced chondrosarcoma. Identification of *NRAS* mutations show that a subset may be particularly sensitive to MEK inhibitors, and these should also be tested in selected patients with chondrosarcoma.

References

1.Bovee JV, Cleton-Jansen AM, Taminiau AH, Hogendoorn PC. Emerging pathways in the development of chondrosarcoma of bone and implications for targeted treatment. Lancet Oncol 2005;6: 599-607.

2.Riedel RF, Larrier N, Dodd L, Kirsch D, Martinez S, Brigman BE. The clinical management of chondrosarcoma. Curr Treat Options Oncol 2009;10: 94-106.

3.Skubitz KM, D'Adamo DR. Sarcoma. Mayo Clin Proc 2007;82: 1409-32.

4.Gelderblom H, Hogendoorn PC, Dijkstra SD, van Rijswijk CS, Krol AD, Taminiau AH, et al. The clinical approach towards chondrosarcoma. Oncologist 2008;13: 320-9.

5.Blume-Jensen P, Hunter T. Oncogenic kinase signalling. Nature 2001;411: 355-65.

6.Zwick E, Bange J, Ullrich A. Receptor tyrosine kinases as targets for anticancer drugs. Trends Mol Med 2002;8: 17-23.

7.Giamas G, Stebbing J, Vorgias CE, Knippschild U. Protein kinases as targets for cancer treatment. Pharmacogenomics 2007;8: 1005-16.

8.Sebolt-Leopold JS, English JM. Mechanisms of drug inhibition of signalling molecules. Nature 2006;441: 457-62.

9.Shao L, Kasanov J, Hornicek FJ, Morii T, Fondren G, Weissbach L. Ecteinascidin-743 drug resistance in sarcoma cells: transcriptional and cellular alterations. Biochem Pharmacol 2003;66: 2381-95.

10.Scully SP, Berend KR, Toth A, Qi WN, Qi Z, Block JA. Marshall Urist Award. Interstitial collagenase gene expression correlates with in vitro invasion in human chondrosarcoma. Clin Orthop Relat Res 2000: 291-303.

11.Gil-Benso R, Lopez-Gines C, Lopez-Guerrero JA, Carda C, Callaghan RC, Navarro S, et al. Establishment and characterization of a continuous human chondrosarcoma cell line, ch-2879: comparative histologic and genetic studies with its tumor of origin. Lab Invest 2003;83: 877-87.

12.Kunisada T, Miyazaki M, Mihara K, Gao C, Kawai A, Inoue H, et al. A new human chondrosarcoma cell line (OUMS-27) that maintains chondrocytic differentiation. Int J Cancer 1998;77: 854-9.

13.van Eijk R, Licht J, Schrumpf M, Talebian Yazdi M, Ruano D, Forte GI, et al. Rapid KRAS, EGFR, BRAF and PIK3CA mutation analysis of fine needle aspirates from non-small-cell lung cancer using allele-specific qPCR. PLoS One 2011;6: e17791.

14.Maira SM, Stauffer F, Brueggen J, Furet P, Schnell C, Fritsch C, et al. Identification and characterization of NVP-BEZ235, a new orally available dual phosphatidylinositol 3-kinase/mammalian target of rapamycin inhibitor with potent in vivo antitumor activity. Mol Cancer Ther 2008;7: 1851-63.

15.Waaijer CJ, de Andrea CE, Hamilton A, van Oosterwijk JG, Stringer SE, Bovée JVMG. Cartilage tumour progression is characterized by an increased expression of heparan sulphate 6O-sulphation-modifying enzymes. Virchows Arch 2012;461: 475-81.

16.Meijer D, de Jong D, Pansuriya TC, van den Akker BE, Picci P, Szuhai K, et al. Genetic characterization of mesenchymal, clear cell, and dedifferentiated chondrosarcoma. Genes Chromosomes Cancer 2012;51: 899-909.

17.Christensen JG, Schreck R, Burrows J, Kuruganti P, Chan E, Le P, et al. A selective small molecule inhibitor of c-

Met kinase inhibits c-Met-dependent phenotypes in vitro and exhibits cytoreductive antitumor activity in vivo. Cancer Res 2003;63: 7345-55.

18.Minkovsky N, Berezov A. BIBW-2992, a dual receptor tyrosine kinase inhibitor for the treatment of solid tumors. Curr Opin Investig Drugs 2008;9: 1336-46.

19.Ji QS, Mulvihill MJ, Rosenfeld-Franklin M, Cooke A, Feng L, Mak G, et al. A novel, potent, and selective insulin-like growth factor-I receptor kinase inhibitor blocks insulin-like growth factor-I receptor signaling in vitro and inhibits insulin-like growth factor-I receptor dependent tumor growth in vivo. Mol Cancer Ther 2007;6: 2158-67.

20.Buck E, Eyzaguirre A, Rosenfeld-Franklin M, Thomson S, Mulvihill M, Barr S, et al. Feedback mechanisms promote cooperativity for small molecule inhibitors of epidermal and insulin-like growth factor receptors. Cancer Res 2008;68: 8322-32.

21.Janku F, Wheler JJ, Westin SN, Moulder SL, Naing A, Tsimberidou AM, et al. PI3K/AKT/mTOR inhibitors in patients with breast and gynecologic malignancies harboring PIK3CA mutations. J Clin Oncol 2012;30: 777-82.

22.Meric-Bernstam F, Akcakanat A, Chen H, Do KA, Sangai T, Adkins F, et al. PIK3CA/PTEN mutations and Akt activation as markers of sensitivity to allosteric mTOR inhibitors. Clin Cancer Res 2012;18: 1777-89.

23.Wullschleger S, Loewith R, Hall MN. TOR signaling in growth and metabolism. Cell 2006;124: 471-84.

24.Bhaskar PT, Hay N. The two TORCs and Akt. Dev Cell 2007;12: 487-502.

25.Efeyan A, Sabatini DM. mTOR and cancer: many loops in one pathway. Curr Opin Cell Biol 2010;22: 169-76.

26.Alessi DR, Andjelkovic M, Caudwell B, Cron P, Morrice N, Cohen P, et al. Mechanism of activation of protein kinase B by insulin and IGF-1. EMBO J 1996;15: 6541-51.

27.Yang J, Cron P, Good VM, Thompson V, Hemmings BA, Barford D. Crystal structure of an activated Akt/protein kinase B ternary complex with GSK3-peptide and AMP-PNP. Nat Struct Biol 2002;9: 940-4.

28.Gingras AC, Raught B, Gygi SP, Niedzwiecka A, Miron M, Burley SK, et al. Hierarchical phosphorylation of the translation inhibitor 4E-BP1. Genes Dev 2001;15: 2852-64.

29.Karim MM, Hughes JM, Warwicker J, Scheper GC, Proud CG, McCarthy JE. A quantitative molecular model for modulation of mammalian translation by the eIF4E-binding protein 1. J Biol Chem 2001;276: 20750-7.

30.Yeh TC, Marsh V, Bernat BA, Ballard J, Colwell H, Evans RJ, et al. Biological characterization of ARRY-142886 (AZD6244), a potent, highly selective mitogen-activated protein kinase kinase 1/2 inhibitor. Clin Cancer Res 2007;13: 1576-83.

31.Vogelstein B, Fearon ER, Hamilton SR, Kern SE, Preisinger AC, Leppert M, et al. Genetic alterations during colorectal-tumor development. N Engl J Med 1988;319: 525-32.

32.Davies H, Bignell GR, Cox C, Stephens P, Edkins S, Clegg S, et al. Mutations of the BRAF gene in human cancer. Nature 2002;417: 949-54.

33.Chow WA. Update on chondrosarcomas. Curr Opin Oncol 2007;19: 371-6.

34.Amary MF, Bacsi K, Maggiani F, Damato S, Halai D, Berisha F, et al. IDH1 and IDH2 mutations are frequent

events in central chondrosarcoma and central and periosteal chondromas but not in other mesenchymal tumours. J Pathol 2011;224: 334-43.

35.Schrage YM, Briaire-de Bruijn IH, de Miranda NF, van Oosterwijk J, Taminiau AH, van Wezel T, et al. Kinome profiling of chondrosarcoma reveals SRC-pathway activity and dasatinib as option for treatment. Cancer Res 2009;69: 6216-22.

36.Garcia-Echeverria C, Sellers WR. Drug discovery approaches targeting the PI3K/Akt pathway in cancer. Oncogene 2008;27: 5511-26.

37.Engelman JA. Targeting PI3K signalling in cancer: opportunities, challenges and limitations. Nat Rev Cancer 2009;9: 550-62.

38.Liu P, Cheng H, Roberts TM, Zhao JJ. Targeting the phosphoinositide 3-kinase pathway in cancer. Nat Rev Drug Discov 2009;8: 627-44.

39.Gingras AC, Raught B, Sonenberg N. Regulation of translation initiation by FRAP/mTOR. Genes Dev 2001;15: 807-26.

40.Grzmil M, Hemmings BA. Translation regulation as a therapeutic target in cancer. Cancer Res 2012;72: 3891-900.

41.Chapuis N, Tamburini J, Green AS, Vignon C, Bardet V, Neyret A, et al. Dual inhibition of PI3K and mTORC1/2 signaling by NVP-BEZ235 as a new therapeutic strategy for acute myeloid leukemia. Clin Cancer Res 2010;16: 5424-35.

42.Nawroth R, Stellwagen F, Schulz WA, Stoehr R, Hartmann A, Krause BJ, et al. S6K1 and 4E-BP1 are independent regulated and control cellular growth in bladder cancer. PLoS One 2011;6: e27509.

43.van Oosterwijk JG, Herpers B, Meijer D, Briaire-de Bruijn IH, Cleton-Jansen AM, Gelderblom H, et al. Restoration of chemosensitivity for doxorubicin and cisplatin in chondrosarcoma in vitro: BCL-2 family members cause chemoresistance. Ann Oncol 2012;23: 1617-26.

44.Manara MC, Nicoletti G, Zambelli D, Ventura S, Guerzoni C, Landuzzi L, et al. NVP-BEZ235 as a new therapeutic option for sarcomas. Clin Cancer Res 2010;16: 530-40.

45.Pansuriya TC, van Eijk R, d'Adamo P, van Ruler MA, Kuijjer ML, Oosting J, et al. Somatic mosaic IDH1 and IDH2 mutations are associated with enchondroma and spindle cell hemangioma in Ollier disease and Maffucci syndrome. Nat Genet 2011;43: 1256-61.

46.Migliardi G, Sassi F, Torti D, Galimi F, Zanella ER, Buscarino M, et al. Inhibition of MEK and PI3K/mTOR suppresses tumor growth but does not cause tumor regression in patient-derived xenografts of RAS-mutant colorectal carcinomas. Clin Cancer Res 2012;18: 2515-25.